Characterisation and performance evaluation of TiSiN & TiAlSiN coatings by RF magnetron sputtering deposition during end milling of maraging steel

To cite this article before publication: Vinay Varghese *et al* 2019 *Mater. Res. Express* in press https://doi.org/10.1088/2053-1591/ab5e74

Characterisation and performance evaluation of TiSiN & TiAlSiN coatings by RF magnetron sputtering deposition during end milling of maraging steel

Vinay Varghese [1], M.R. Ramesh [1] and D. Chakradhar [2], Habibuddin Shaik [3]

[1] Department of Mechanical Engineering, National Institute of Technology Karnataka, Surathkal, Mangalore, India.

[2] Department of Mechanical Engineering, Indian Institute of Technology, Palakkad, India.

[3] Centre for Nanomaterials and MEMS, Nitte Meenakshi Institute of Technology, Bangalore, India

Abstract

Monolayer nanostructured thin films of TiSiN & TiAlSiN were deposited on WC-Co milling inserts using RF magnetron sputtering for metal cutting. The alloy targets of TiSi (80/20 at. %) & TiAlSi (34/56/10 at. %) were used for the deposition in an Ar + N atmosphere. The deposition time and parameters are optimized to develop a uniform and homogenous coating. The mechanical and metallurgical properties are characterized to analyze the wear resistance of the coating. The machinability studies on MDN 250 maraging steel is carried out using TiSiN and TiAlSiN coated WC-Co inserts under dry and wet environment. The machining responses such as surface roughness, cutting force, tool wear and tool life are analyzed by varying spindle speed. The results showed that TiAlSiN coating had a higher wear resistance and machining performance compared to the TiSiN coating owing to the high hardness and plasticity index of the coating.

Keywords: Magnetron sputtering; thin films; TiSiN; TiAlSiN; tool wear; surface roughness.

Introduction

Maraging steel belongs to a class of ultrahigh strength martensitic steel whose strength is due to precipitation of intermetallic compounds. The ultra-high-strength coupled with fracture toughness and minimum weight requirement while ensuring high reliability makes maraging steel ideal candidate for applications in aeronautical and aerospace. Applications of maraging steel include rocket motor cases, submarine hulls, landing gears and cryogenic missiles [1,2]. The high strength and hardness makes maraging steel difficult to machine material [3–5]. Excessive tool wear, high heat generation, high power consumption, larger cutting forces, poor surface quality and/or difficulties in chip formation are some of the difficulties faced while machining maraging steel. The high wear resistance and thermally stable behaviour of coated tools at high temperatures help to improve the tool life of the cutting tool. The use of coated tools improves the productivity and surface quality requirement while machining hard materials like maraging steel. The productivity and surface quality are the two important aspects which affect the metal cutting industry. The dry machining is considered as the future of the sustainable machining process as the conventional cutting fluids are causing a lot of problems in recycling, disposal, operator safety and environmental pollution. The cutting

temperature as a result of dry machining is very high. The need for coatings to withstand the high cutting temperature is a challenge faced by cutting tool manufacturers.

The coatings were first used for cutting tool applications back in the 1980s. Magnetron sputtering, cathodic arc, plasma enhanced chemical vapour deposition (PECVD), large area filtered arc deposition (LAFAD) were some of the methods used for coating cutting tools. PVD techniques like magnetron sputtering, cathodic arc and LAFAD were considered more over CVD as the former avoided precursor gases that is not suitable with corrosion, fire and environmental hazards [6,7]. Magnetron sputtering has better adhesion and tribological properties compared to cathodic arc deposition (CAD). The later also forms macro- droplets which increases the surface roughness of coatings [8]. The first commercial coating was a titanium nitride (TiN) based physical vapour deposition (PVD) coating developed for high-speed steel drills [9]. The conventional nitride coatings could not meet the demands of dry cutting technology. It is desirable for coatings to have high hardness, low friction and high-temperature oxidation resistance [10]. Nanocomposite coatings of MoN/CrN, TiSiN, and TiAlSiN were some of the alternatives due to their extensive mechanical properties. It is found that the addition of Al & Si into TiN coatings can enhance the mechanical properties of titanium nitride coatings [11]. TiAlSiN and TiSiN coatings are not only good in mechanical properties but also exhibited low thermal conductivity which is desirable for dry machining.

TiAlSiN coatings have drawn attention from many researchers because of their high hardness, adhesion strength and better oxidation resistance at high temperatures [12]. According to Fuentes [13], TiAlSiN coating consists of (Ti,Al,Si)N where Aluminium and Silicon replace Titanium atoms in an fcc crystalline lattice, depending on the stoichiometry. It is Veprek (5,6,13), who studied continuously on nanocomposite coatings of TiN, TiAlN, TiSiN and TiAlSiN respectively. It is reported that TiAlSiN coating consisted of nanocrystalline TiAlN phase and amorphous Si_3N_4 phase, where former is wrapped in later. Veprek [15] has previously reported about the existence of Silicon nitride (Si_3N_4) as amorphous phase at deposition temperatures below 700-800° C. The microstructure of coating is completely dependent on the concentration of each element present and addition of Si to TiAlN has clearly resulted in the refinement of grains and increase in hardness as reported by some of the researchers [16,17]. The researchers also reported that an increase in Al content decreased grain size and increased thermal stability and oxidation resistance [18]. The Ti atoms in TiN lattice is replaced by Al atoms and resulted in more lattice distortion and residual stress in the coatings. TiSiN coatings also possess excellent properties as that of TiAlSiN coatings for

cutting tool applications. The formation of dense SiO_2 tribo layer improves oxidation resistance of TiSiN coatings at high temperature [19]. The microstructure of TiSiN is also similar to TiAlSiN coating, consisting of nano crystalline TiN phase and amorphous Si_3N_4 phase. TiSiN and TiAlSiN coatings are some of the widely used tribological coatings for cutting tool applications especially high-speed machining under dry environment. Bouzakis [20] and Chen [21] reported a decrease in milling performance of TiSiN coating due to high stress and weak adhesive bonding between substrate and coating. Although mechanical properties and characteristics of coatings are well studied, the tribological behaviour and wear characteristics are still not clear due to the complex wear behaviour of hard coatings. An attempt has been made to study the characteristics of TiSiN and TiAlSiN coatings during end milling of maraging steel under dry and wet environments. Milling is a cutting process in which coatings require high adhesive strength and wear resistance as cutting force and thermal stresses are very high [22]. Most of the researchers have studied the microstructure and mechanical properties of the coatings giving less importance to machining aspects. This research not only deals with characteristics of the coatings but also the mechanical behaviour during end milling of maraging steel under dry and wet environment.

The present study deals with the development of nanocomposite coatings of TiSiN and TiAlSiN on tungsten carbide milling inserts using RF magnetron sputtering technique. The mechanical and metallurgical characterisation of coatings is carried out using SEM/EDS, XRD, Raman spectroscopy and nanoindentation to determine coating thickness, chemical composition, phase change, peak shift, hardness and Young's modulus. The end milling performance of coated inserts is carried out by varying spindle speed. The surface roughness, cutting force and tool wear characteristics is analysed to evaluate machining performance of TiSiN and TiAlSiN coated inserts.

Materials and methods

A commercially available tungsten carbide inserts (H15) purchased from Seco India Ltd is used for the coating process. Samples were ultrasonically cleaned using isopropyl alcohol (IPA) for 15 minutes at ambient temperature. The sample was placed in the sputtering unit mounted to an aluminium holder rotating at a speed of 20 rpm. The magnetron sputtering unit used is supplied by V.R. Technologies, Bangalore. The chamber was evacuated to a base pressure of about 1.0×10^{-3} Pa. The target alloys of TiSi (80/20 at. %) and TiAlSi (54/36/10 at. %) is procured from Plansee Composite Materials GmbH, Germany. High purity argon gas was

supplied to the chamber at a flow rate of 30 sccm to achieve a chamber pressure of 0.6 Pa. The pre-sputtering was carried out for 20 minutes keeping the bias voltage and current at 433V and 0.21 A. The nitrogen partial pressure was subsequently adjusted to 3.35 Pa and a flow rate of 16 sccm. The argon gas pressure was reduced to 20 sccm. The deposition time of TiSiN and TiAlSiN coatings was 120 minutes and 150 minutes. Figure 1 shows the experimental setup of magnetron sputtering of TiSiN or TiAlSiN coating during the process.

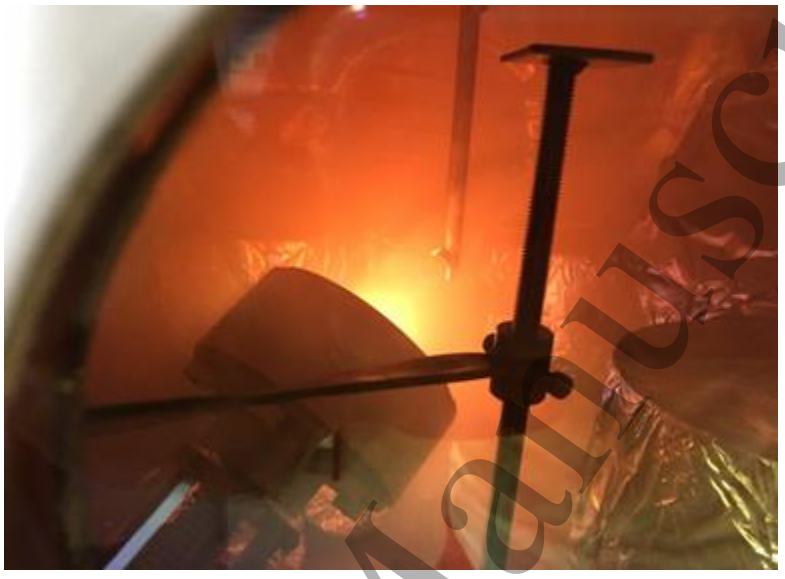

Figure 1. Magnetron sputtering of TiAlSiN or TiSiN coatings.

Table 1. Physical and mechanical properties of MDN 250 maraging steel.

Density (g/cm^3)	**Yield tensile strength**	**Ultimate tensile strength**	**Young's modulus**	**Hardness (aged)**	**Thermal conductivity**	**Coefficient of thermal expansion**	**Melting point**
	GPa	**GPa**	**GPa**	**HRC**	**W/mK**		**°C**
8.1	1.78	1.85	210	50	25.5	11.3x10-6	1413

Table 2. Chemical composition of MDN 250 maraging steel.

Elements	Ni	Co	Al	Mo	Mn	Ti	Si	C	Fe
Nominal composition (At. %)	18.5	8.5	4.17	4.8	0.05	0.4	0.05	0.01	Bal

The elemental constituents of the coatings were identified using Zeiss Gemini SEM 500. The crystal structures in the uncoated and coated tools are determined by XRD analysis using Bruker Model: D8 Advance. The Hardness and Young's Modulus of the coatings are measured by using Microtrac Model: Blue Wave. A peak load of 50 mN is applied for the nanoindentation test to eliminate the effect on measured hardness due to the substrate, by corroborating that resulting pierced depth is within the 10% of coating thickness; around 20 indentations are performed on each sample for ensuring the accuracy of the results. Calo-tester by Anton Paar, USA is used to measure the thickness of coated cemented carbides.

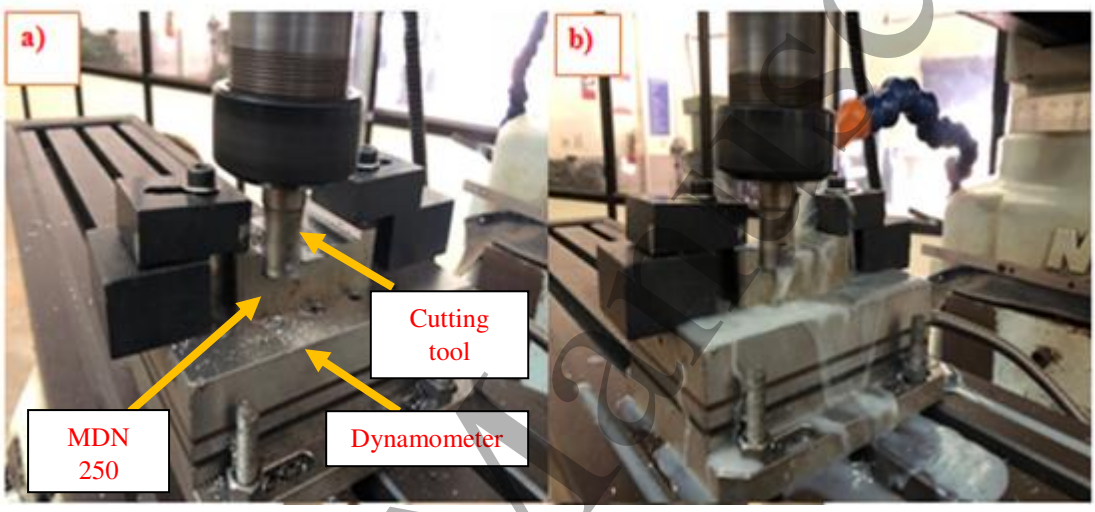

Figure 2. Experimental setup for end milling of MDN 250 maraging steel a) Dry environment b) Wet environment

Table 3. Cutting parameters used for end milling of maraging steel.

Description	Parameters
Spindle speed (rpm)	270, 350 & 540
Cutting tool	Uncoated, AlTiN & AlCrN coated tool
Feed rate (mm/min)	58
Depth of cut (mm)	0.3
Cutting environment	Dry & Wet

A conventional three-axis vertical milling machine NAMMILL X6325 is used for milling trials. The experimental setup for dry and wet end milling is presented in Figure 2. The end mill cutter used is produced by Seco with 20 mm diameter and two flutes. Annealed maraging steel MDN 250 from MIDHANI Ltd. India is used to carrying out machinability studies. The mechanical properties and chemical composition of MDN 250 are illustrated in Table 1 and 2. An emulsion type of cutting fluid is used as a wet coolant and is prepared by mixing soluble oil with water at a proportion of 1:20. The coolant is flooded into the machining

zone at a pressure of 1 bar and 6 L/min flow rate. The cutting parameters used in the experiment is presented in Table 3. The tool life of the cutting tool is determined in accordance with ISO 8688-2:1989. The maximum width of flank wear for tool life criterion is kept at 0.5 mm. The width of flank wear is measured at an interval of 4 passes (5 minutes) using an optical microscope. A quartz three component dynamometer Kistler 9257B is used for measuring cutting forces in three different directions. The average surface roughness (R_a) is measured using a Talysurf SJ 301 with a cut off length of 4 mm at 6 different locations.

Results and discussion

The microstructure of TiAlSiN & TiSiN coatings is shown in Figure 3. The average coating thickness is found to be 1.2 µm for TiAlSiN coating and 1.6 µm for TiSiN coating from the cross-section of the microstructure. The surface morphology of coatings revealed that a homogenous and uniform coating consisting of spherically shaped clusters has been formed using a magnetron sputtering technique. The elemental composition of coatings are summarized in Table 4 and illustrated in Figure 4. The EDS analysis shows the presence of elements like Ti, Al, Si, N & O respectively. Figure 5 presents the XRD analysis of coatings The XRD patterns of coatings show the presence of nanocrystalline TiAlN in TiAlSiN coatings and TiN in TiSiN coatings. The XRD analysis of coatings showed the presence of TiN & substrate phase in TiSiN and TiAlN, TiN phase in TiAlSiN. The TiAlSiN structure mainly consists of amorphous Si_3N_4 phase and nano-crystalline TiAlN phase. The amorphous phase cannot be seen in the XRD analysis but the presence of Silicon is evident from EDS results. The addition of aluminium and silicon into the nano-crystalline TiN has changed the morphology of TiSiN & TiAlSiN coatings from columnar to non-columnar structure [19]. The change from columnar to non-columnar structure helps in improving the mechanical properties of the coating as the columnar structure suffers from weaker bonding between the columns. The microstructure also revealed that TiAlSiN coating has a denser and uniform distribution of particles compared to TiSiN coating. The reduced intensity of TiN phase in TiSiN & TiAlSiN coating is an indication of decreased grain size [23]. Also, the broadening of TiAlN peak in TiAlSiN coating proves the grain size of TiAlSiN coating (35 nm) is much smaller compared to TiSiN coating (72 nm). The coating thickness and surface roughness of coatings are presented in Table 5. The surface roughness of TiSiN coating (0.323 µm) is quite high compared to TiAlSiN coating (0.242 µm).

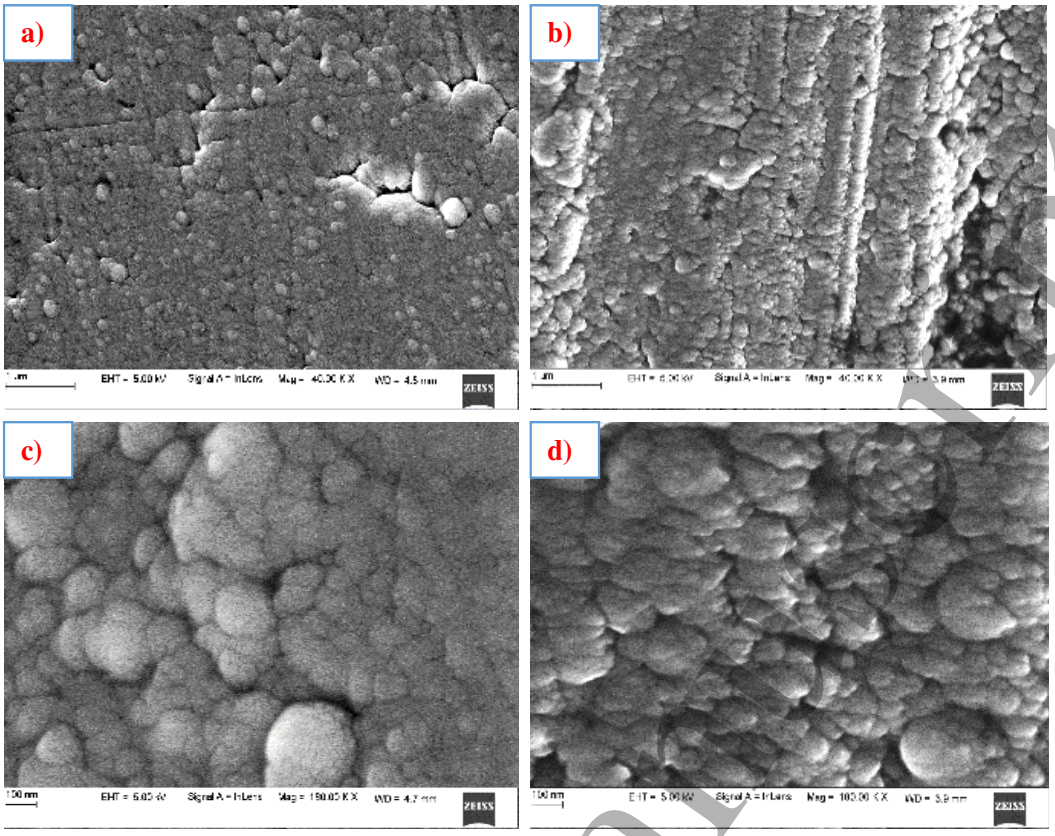

Figure 3. Microstructure of coatings a) TiAlSiN (1.2 µm thick) at 40 K X & b) TiSiN (1.6 µm thick) at 40 K X c) TiAlSiN at 180 K X d) TiSiN at 180 K X.

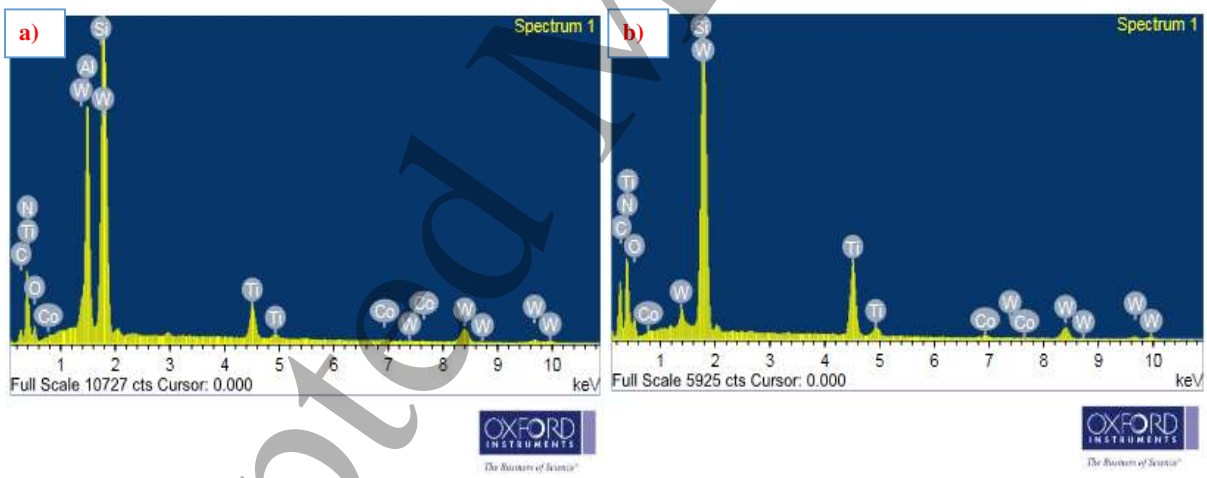

Figure 4. EDS analysis of a) TiAlSiN b) TiSiN coatings.

Table 4. Chemical composition of coatings from EDS analysis.

Designation	Ti (At. %)	Al (At. %)	Si (At. %)	N (At. %)	O (At. %)
TiAlSiN	4.76	13.82	3.14	59.96	18.32
TiSiN	16.58	-	4.94	67.46	11.02

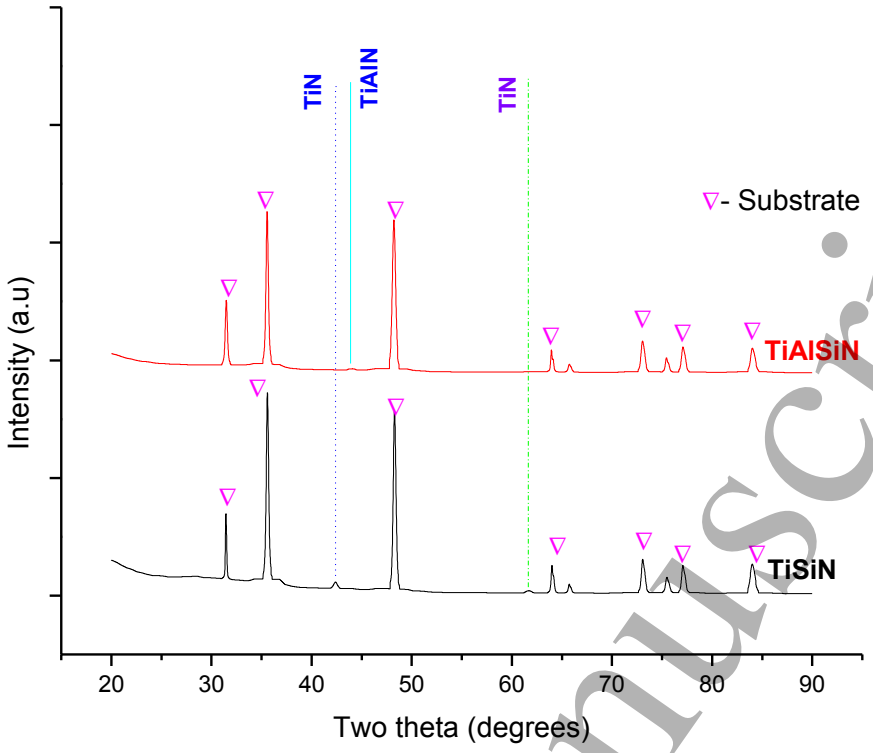

Figure 5. XRD patterns of TiAlSiN & TiSiN coated WC-Co inserts.

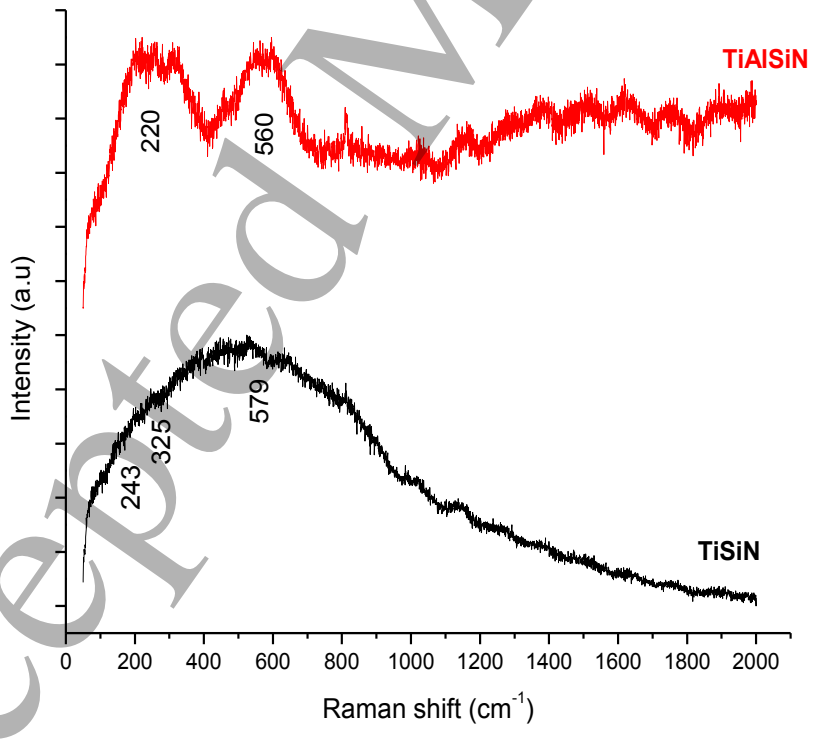

Figure 6. Raman spectroscopy of TiAlSiN & TiSiN coatings.

Figure 6 indicates the raman spectroscopy of TiSiN and TiAlSiN coatings. The raman spectroscopy of TiSiN shows one broad band centred approximately at 579. This band corresponds to the optic and acoustic modes in the 100 cm^{-1}region. Scattering of heavy metal (Ti) ions results in the acoustic mode and scattering of light element (N) ions results in optic mode. Similarly, for TiAlSiN coating, raman spectra consist of two bands centred approximately at 220 & 560. The study by Barshilla [24] found the two bands in the raman spectra of TiAlSiN coatings represent the optic and acoustic modes. The bands between the region 150 and 350 cm^{-1} represent the acoustic mode due to the scattering of heavy metal (Ti, Al) ions and the bands between the region 400 and 650 cm^{-1} represent optic mode due to scattering of light metal (N) ions.

Table 5. Micro mechanical characteristics of TiAlSiN and TiSiN coatings.

Coatings	**Average thickness**	**Surface roughness**	**Hardness (H)**	**Young's modulus (E)**	**H/E Ratio**	**H^3/E^2 Ratio**	**Plasticity index,[1-x(H/E)]**
	µm	**µm**	**GPa**	**GPa**		**GPa**	
TiAlSiN	1.2	0.242	32 ± 2.1	380±5.6	0.084	0.227	0.975
TiSiN	1.6	0.323	28 ± 1.8	285±3.1	0.098	0.185	0.970

The mechanical properties of coatings are summarized in Table 5. The micromechanical characteristics of coatings revealed that hardness and Young's modulus is greater for TiAlSiN coating (32 GPa & 380 GPa) compared to TiSiN coating (28 GPa & 285 GPa). The increased Si percentage in TiSiN coatings resulted in non-columnar structure, higher mechanical properties and better bonding between atoms [25]. The measure of resistance to local plastic deformation is known as hardness. The hardness and toughness are the key aspects to evaluate and predict the tribological aspects for engineering applications [26]. High hardness and toughness is vital for the wear resistance of coatings under severe cutting conditions [27]. The hardness is directly correlated to slipping of dislocation and nucleation. The high Si content in the TiSiN reduced the grain size of the particle. The plastic deformation mechanism happening in smaller grain size are grain boundary sliding and not dislocation sliding. The dislocations are generally absent in the case of TiSiN coating due to smaller grain size. The high hardness of TiSiN coating is due to the high bonding energy of Si-

Ti and Si-N bonds in the grain boundary which resisted the grain sliding [28]. The strong interphase boundary between nanocrystalline TiAlN and amorphous Si_3N_4 phase with high cohesive energy combined with grain size refinement should be the reason for the high hardness of TiAlSiN coating. In addition, the solution hardening incorporation of Al can also be the reason for higher hardness. The small grain size of TiAlSiN hinders the dislocation movement and dislocations are generally absent at very small grains resulting in high hardness. The quaternary coating (TiAlSiN) has better hardness than ternary coating (TiSiN) because the interface phase (Si_3N_4) retards the decomposition phase of TiAlN phase [29]. Generally cutting tools requires higher values of hardness in order to avoid the drastic tool wear. Higher H/E values are obtained for TiSiN coating which is a measure of plasticity. The load-bearing capacity (H^3/E^2) of TiAlSiN coating (0.227 GPa) is found to be higher than TiSiN coating (0.185 GPa), which indicates the plastic deformation resistance and fracture toughness is more for the former. In general tribological conditions, the higher H//E values result in lower wear. But the hardness and H/E ratio are inadequate to evaluate the performance of the coating in the severe cutting conditions like high-speed machining [30]. The plasticity index is a measure of toughness and is more reliable to evaluate the actual cutting conditions. The TiAlSiN coating has higher plasticity index compared to the TiSiN coating. The plasticity index of the coating is correlated with the tool life in end milling of hardened steel [31].

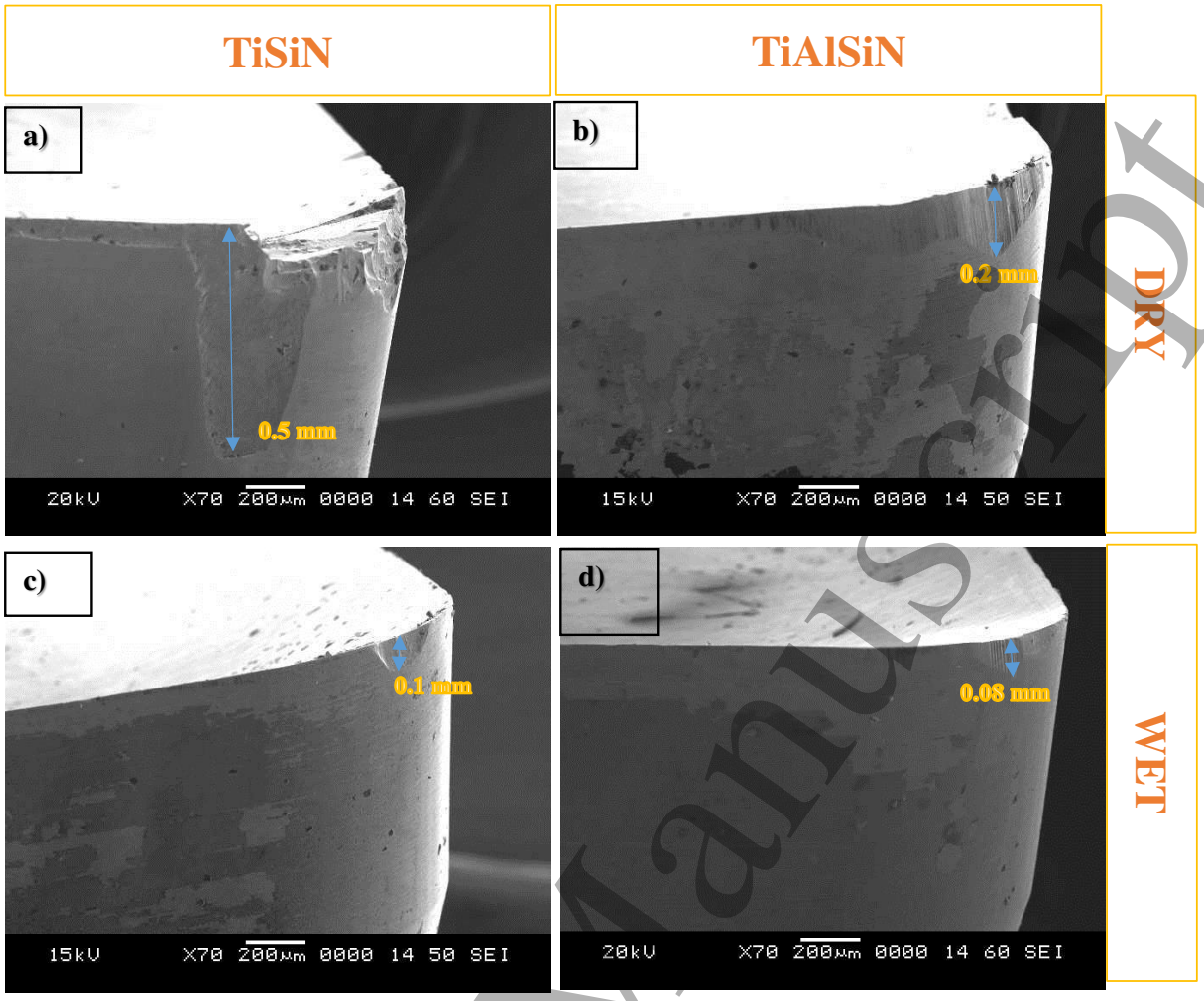

Figure 7. Flank wear of coated inserts at a spindle speed of 540 rpm a) TiSiN coated inert under dry environment b) TiAlSiN coated insert under dry environment c) TiSiN coated insert under wet environment d) TiAlSiN coated insert under wet environment

The dominant tool wears observed in the coated inserts during dry and wet milling is flank wear & chipping, not crater wear at rake face. The SEM image of flank wear during dry and wet milling at a spindle speed of 540 rpm is shown in Figure 7. The flank wear progression followed a V pattern due to the high abrasive wear while machining. The best wear performance is by TiAlSiN coated carbide tools during wet end milling. This is because of the good mechanical properties of TiAlSiN coating like high hardness and toughness which helped in resisting wear. The dry environment machining involves high thermal stress due to the high heat generated. The high heat generated to deteriorate the adhesion between coating and substrate and results in peeling of coating. The substrate is exposed after this and leads to fracture of the cutting tool. The abrasive wear is more during dry machining and a rapid progression of flank wear reduces the tool life. The tribo oxide films like TiO_2, SiO_2, Al_2O_3 & $Al_xSi_yO_z$ protects the TiAlSiN coating, whereas TiO_2 & SiO_2 protects the TiSiN coating. The

presence of oxygen is evident from the EDS results (Figure 4) of coatings and the formation of oxide films on coatings is expected. The TiO_2 & SiO_2 protective layer in the TiSiN coating is comparatively weak when compared to strong oxide layers of Al_2O_3 and $Al_xSi_yO_z$ in TiAlSiN coating [32]. The alumina and silica tribo films formed on the coatings has played a vital role in increasing the wear resistance of TiAlSiN coating [13]. The TiSiN coating and TiAlSiN coating is fractured more under dry environment than under a wet environment. The abrasive wear is less under a wet environment as the cutting temperature dropped, better lubrication and chip removal also helped. The adhesion and built up edge formation is also less during wet machining giving a better surface finish. The microchipping and peeling of coating also are observed in coatings under a wet environment. The TiAlSiN coatings had a better wear resistance and tool life under a wet environment. The results were in accordance with studies by Yuan et al. [27] where TiAlSiN coating had higher tool life compared to TiSiN and TiCrSiN coatings. The pin hole defects affected the wear resistance and tool life of TiSiN coatings even though having good mechanical properties.

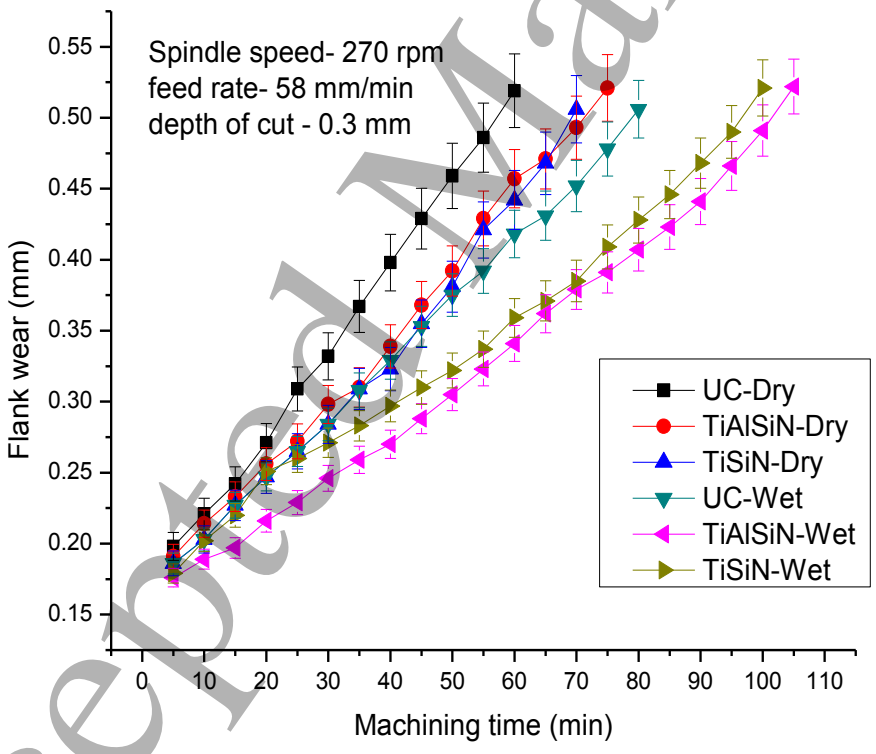

Figure 8. Progression of flank wear of different cutting tool at a spindle speed of 270 rpm

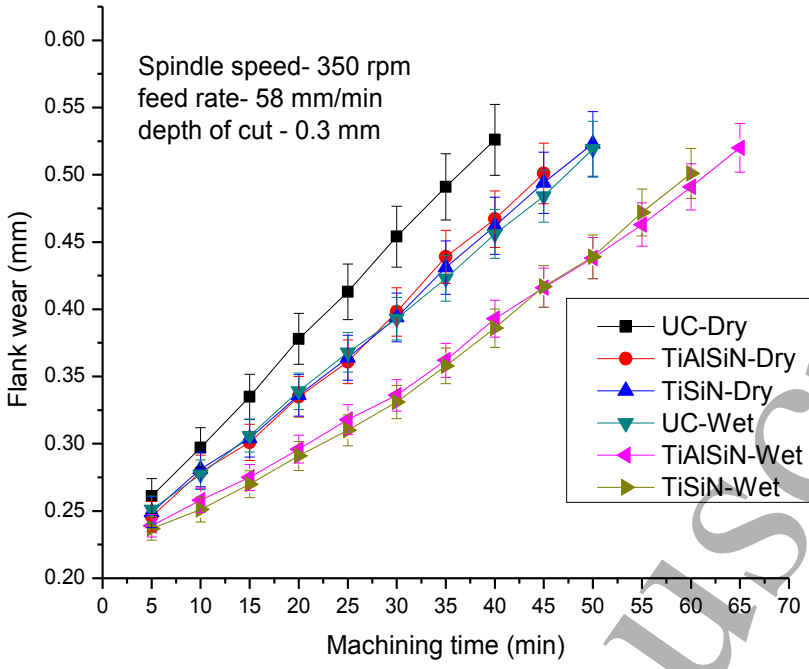

Figure 9. Progression of flank wear of different cutting tool at a spindle speed of 350 rpm.

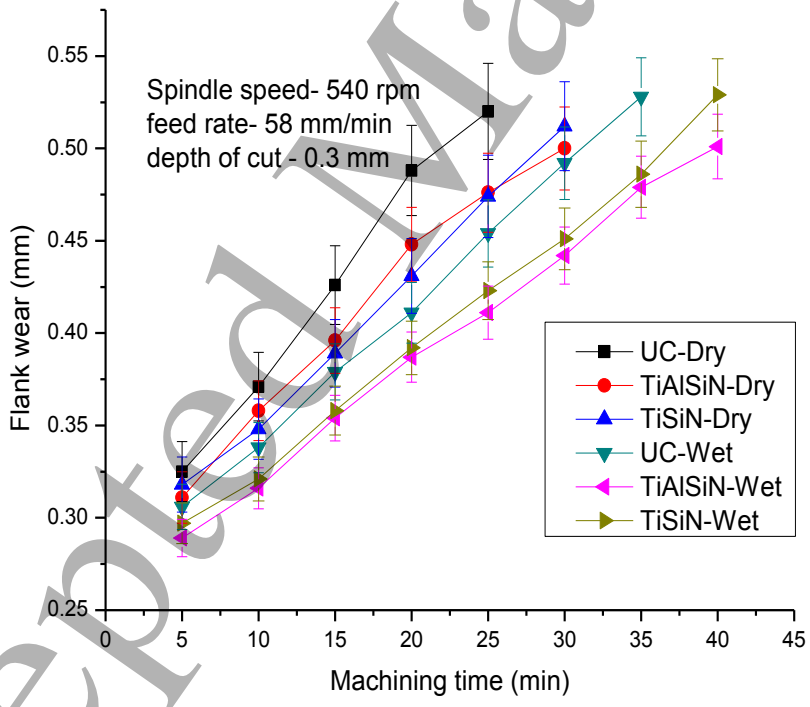

Figure 10. Progression of flank wear of different cutting tool at a spindle speed of 540 rpm.

Table 6. Tool life of cutting tools at different spindle speed and cutting environments

Spindle speed	Tool life (min)					
	UC	TiAlSiN	TiSiN	UC	TiAlSiN	TiSiN
(rpm)	Dry	Dry	Dry	Wet	Wet	Wet
270	59	71	70	80	102	96
350	37	45	46	48	61	60
540	22	30	28	32	40	37

The progression of flank wear of coated and uncoated tools during machining under a dry and wet environment at a spindle speed of 270, 350 & 540 rpm taken at an interval of 5 minutes is presented in Figures 8, 9 & 10 respectively. The tool life is estimated on the basis of maximum flank wear criteria of 0.5 mm (ISO 8688-2:1989) and the same is presented in Table 6. The coated tools resisted the flank wear for a long time compared to uncoated tools and extended their tool life. The cutting tools had a better flank wear resistance during lower spindle speeds and progression of flank wear increased during higher spindle speeds. Thus resulting in a better tool life during lower spindle speeds. The cutting tool is worn fast during cutting under dry machining and resulted in lesser tool life compared to wet machining. TiAlSiN coated tools had a better wear resistance compared to the TiSiN coated tool and resulted in maximum tool life of 102 minutes during wet machining at a spindle speed of 270 rpm. The formation of tribo films of Al_2O_3 and $Al_xSi_yO_z$ in TiAlSiN coating protects the cutting tool from the progression of flank wear and results in higher tool life. The wet environment reduces the cutting temperature and provides better lubrication and cooling compared to a dry environment. The reduction in cutting temperature reduces the thermal stresses and fatigue associated with insert and extends tool life. The cutting temperature is less during lower spindle speeds and reduces tool wear.

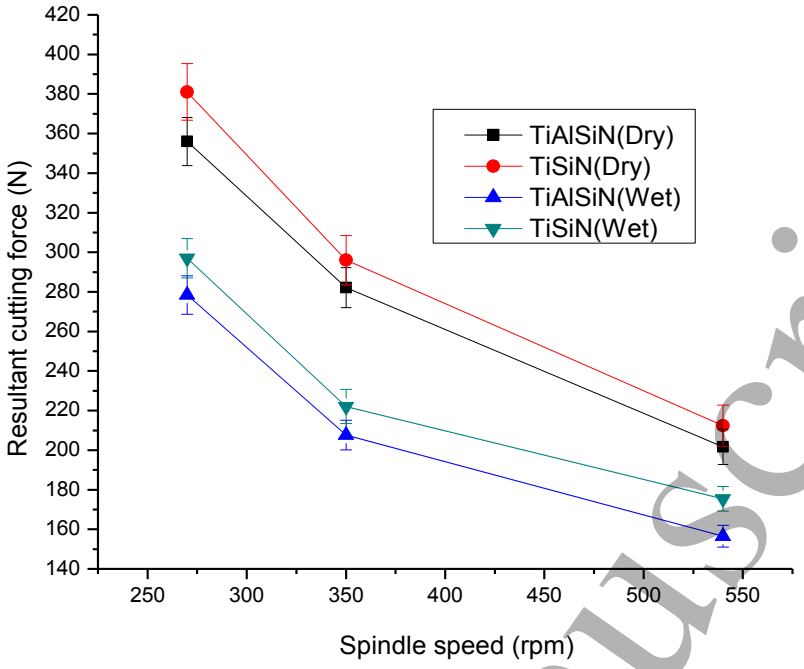

Figure 11. Variation of resultant cutting force with spindle speed during dry and wet milling using coated carbide inserts.

The resultant cutting force (F_R) is used to analyse the cutting force while machining [22]. The cutting force is directly correlated with power consumption during machining. So it is recommended to have a lower cutting force while machining to reduce the power consumption. It is also a measure of machinability index. Figure 11 presents the variation of resultant cutting force while machining at a spindle speed of 270, 350 & 540 rpm using coated carbide tool under dry and wet environment. It is observed that TiAlSiN coated tools had lower cutting force than TiSiN coated tools under dry and wet environment. The cutting force decreased as the spindle speed increased, the chatter and vibration are more at lower spindle speed. The high hardness, Young's modulus and toughness of TiAlSiN coatings improved the wear resistance of the coating and resulted in a lower cutting force. The uniform and dense microstructure along with reduced grain size also attributed to a reduction in cutting force. The higher friction coefficient of TiSiN coatings also resulted in an increase in cutting forces [27]. The cutting force is high during machining under dry environment as the high cutting temperature increased the thermal stress and resulted in the fracture of the coating. The higher wear resistance of TiAlSiN coating helped to extend the tool life and reduce the cutting force even in the dry environment. The TiSiN coating had a higher wear rate and increased the cutting force while machining. The better lubrication and cooling effects of a wet environment not only reduced the wear rate but also the cutting force. TiAlSiN coating had a better performance

than TiSiN coatings and major wear mechanisms like abrasive wear, BUE formation and fracture of coatings eliminated during wet machining. The tribo protective layers like alumina (Al_2O_3) & silica (SiO_2) also helped TiAlSiN coated tools to reduce friction coefficient and cutting force.

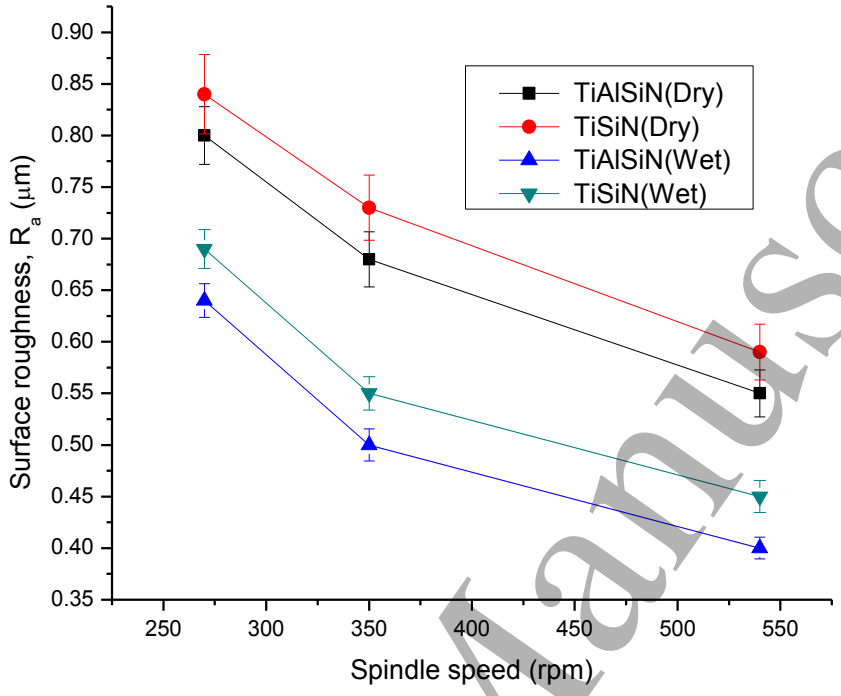

Figure 12. Variation of surface roughness with spindle speed during dry and wet milling using coated carbide inserts.

The surface roughness is a measure of surface integrity which affects the fatigue life of the components produced. The lower surface roughness will give a better finish and protect the component from fatigue failure. The surface roughness of maraging steel after machining at different spindle speed using TiSiN and TiAlSiN coated tools has been presented in Figure 12. It can be observed that the surface roughness reduced as the spindle speed increased and TiAlSiN coated tools produced a better surface finish compared to TiSiN coated tools. The wet environment helped to reduce the surface roughness of the machined surface to a large extent as seen in the figure. As the spindle speed increased, the cutting temperature also increased and resulted in the thermal softening of the workpiece. It also helped in removing the surface discontinuities and other defects along with easy chip removal. The high spindle speed also reduced the chatter and vibration of the cutting tool thereby leaving fewer tool marks on the workpiece surface. The high hardness and plasticity index of TiAlSiN coating helped to extend the wear resistance and tool life of the cutting inserts. The high wear resistance of TiAlSiN

coated tool improved the surface finish of machined workpiece compared to the TiSiN coated inserts. The fractured tool leaves more marks on the workpiece surface and it is desired to have better wear resistance for better surface finish. The alumina and silica tribo films are the reason for the wear protection of the TiAlSiN coatings and better finish of maraging steel. The conventional wet coolant helped in reducing the cutting temperature and provided better lubrication compared to the dry cutting. The use of coolant also resulted in easy chip disposal and reducing tool marks on the machined surface. The employment of coolant improved the chip breakability of the coated tool and reduced the coefficient of friction. The results were in accordance with previous works [33].

Conclusions

The TiSiN & TiAlSiN coatings are well deposited on WC-Co milling inserts using PVD magnetron sputtering technique with TiSi (80/20) and TiAlSi (54/36/10) targets. The microstructure and mechanical properties of coatings were studied along with the mechanical performance of coatings during end milling of maraging steel by varying spindle speed. The following conclusions are drawn from the study:

i. The microstructure revealed that coatings were uniform and densely distributed and formed a nanocrystalline structure of TiN & amorphous Si_3N_4 phase in TiSiN coating and nanocrystalline structure of TiAlN & amorphous Si_3N_4 phase in TiAlSiN coating.
ii. TiAlSiN coating had higher hardness and Young's modulus than TiSiN coating. Also, the load bearing capacity (H^3/E^2 ratio) and plasticity index of the coating of TiAlSiN coating is also higher for TiSiN coating.
iii. The TiAlSiN coating had better wear resistance than TiSiN coating due to good mechanical properties and resulted in tool life enhancement.
iv. The highest tool life observed during end milling using TiAlSiN coating is 102 minutes at a spindle speed of 270 rpm under a wet environment.
v. The coatings performed better under wet environment than in dry environment and the abrasion wear, BUE formation and the fracture was more during dry machining. While adhesion wear, coating peels off and microchipping is observed more during wet machining.
vi. The cutting force and surface roughness is higher while machining using TiSiN compared to TiAlSiN coated tool.

Acknowledgements

The PVD coatings were developed in Centre for Nanomaterials and MEMS Laboratory (CNM Lab), Nitte Meenakshi Institute of Technology, Bangalore. The authors also acknowledge the Centre for Nano Science and Engineering (CeNSE), Indian Institute of Science, Bangalore for characterization and other support.

References

[1] Viswanathan UK, Dey GK, Asundi MK 1993 Precipitation hardening in 350 grade maraging steel Metall Trans A. 24 2429–42. doi:10.1007/BF02646522.

[2] Li B, Ding Z, Xiao J, Liang SY 2015 Maraging steel 3J33 phase transformation during micro-grinding Mater Lett.164 217–20. doi:10.1016/j.matlet.2015.10.162.

[3] Venkata Ramana P, Madhusudhan Reddy G, Mohandas T, Gupta AVSSKS 2010 Microstructure and residual stress distribution of similar and dissimilar electron beam welds - Maraging steel to medium alloy medium carbon steel Mater Des. 31 749–60. doi:10.1016/j.matdes.2009.08.007.

[4] Varghese V, Ramesh MR, Chakradhar D 2019 Influence of deep cryogenic treatment on performance of cemented carbide (WC-Co) inserts during dry end milling of maraging steel J Manuf Process. 37 242–50. doi:10.1016/j.jmapro.2018.11.030.

[5] Varghese V, Ramesh MR, Chakradhar D 2019 Experimental investigation of cryogenic end milling on maraging steel using cryogenically treated tungsten carbide-cobalt inserts Int J Adv Manuf Technol.

[6] Veprek S, Reiprich S. A 1995 concept for the design of novel superhard coatings. Thin Solid Films. 268 64–71.

[7] Veprek S, Jilek M 2002 Super- and ultrahard nanacomposite coatings: Generic concept for their preparation, properties and industrial applications Vacuum. 67 443–9. doi:10.1016/S0042-207X(02)00229-4.

[8] Sanchette F, Ducros C, Schmitt T, Steyer P, Billard A 2011 Nanostructured hard coatings deposited by cathodic arc deposition: From concepts to applications Surf Coatings Technol. 205 5444–53. doi:10.1016/j.surfcoat.2011.06.015.

[9] Inspektor A, Salvador PA 2014 Architecture of PVD coatings for metalcutting applications: A review Surf Coatings Technol. 257 138–53. doi:10.1016/j.surfcoat.2014.08.068.

[10] Ma Q, Li L, Xu Y, Ma X, Xu Y, Liu H 2016 Effect of Ti content on the microstructure and mechanical properties of TiAlSiN nanocomposite coatings Int J Refract Met Hard Mater. 59 114–20. doi:10.1016/j.ijrmhm.2016.06.005.

[11] Varghese V, Chakradhar D, Ramesh MR 2018 Micro-mechanical characterization and wear performance of TiAlN / NbN PVD coated carbide inserts during End milling of AISI 304 Austenitic Stainless Steel. Mater Today Proc. 5 12855–62. doi:10.1016/j.matpr.2018.02.270.

[12] Ma Q, Li L, Xu Y, Gu J, Wang L, Xu Y 2017 Effect of bias voltage on TiAlSiN nanocomposite coatings deposited by HiPIMS. Appl Surf Sci. 392 826–33. doi:10.1016/j.apsusc.2016.09.028.

[13] Fuentes GG, Almandoz E, Pierrugues R, Martínez R, Rodríguez RJ, Caro J, et al 2010 High temperature tribological characterisation of TiAlSiN coatings produced by cathodic arc evaporation Surf Coatings Technol. 205 1368–73. doi:10.1016/j.surfcoat.2010.09.004.

[14] Veprek S, Zhang RF, Veprek-Heijman MGJ, Sheng SH, Argon AS 2010 Superhard nanocomposites: Origin of hardness enhancement, properties and applications Surf Coatings Technol. 204 1898–906. doi:10.1016/j.surfcoat.2009.09.033.

[15] Veprek S, Veprek-Heijman MGJ 2012 Limits to the preparation of superhard nanocomposites: Impurities, deposition and annealing temperature Thin Solid Films. 522 274–82. doi:10.1016/j.tsf.2012.08.048.

[16] She-quan W, Kang-hua C, Li C 2011 Effect of Al and Si additions on microstructure and mechanical properties of TiN coatings. J Cent South Univ Technol. 18 310–3. doi:10.1007/s11771−011−0696−4.

[17] Wang SQ, Chen L, Yang B, Chang KK, Du Y, Li J, et al 2010 Effect of Si addition on microstructure and mechanical properties of Ti – Al – N coating RMHM. 28 593–6. doi:10.1016/j.ijrmhm.2010.05.001.

[18] Chen L, Du Y, Wang AJ, Wang SQ, Zhou SZ 2009 Effect of Al content on microstructure and mechanical properties of Ti – Al – Si – N nanocomposite coatings. Int J Refract Met Hard Mater. 27 718–21. doi:10.1016/j.ijrmhm.2008.12.002.

[19] Cheng YH, Browne T, Heckerman B 2009. Nanocomposite TiSiN coatings deposited by large area filtered arc deposition. J Vac Sci Technol A Vacuum, Surfaces, Film. 27 82. doi:10.1116/1.3043460.

[20] Bouzakis KD, Skordaris G, Gerardis S, Katirtzoglou G, Makrimallakis S, Pappa M, et al. 2009 Ambient and elevated temperature properties of TiN, TiAlN and TiSiN PVD films and their impact on the cutting performance of coated carbide tools. Surf Coatings Technol. 204 1061–5. doi:10.1016/j.surfcoat.2009.07.001.

[21] Chen L, Du Y, Wang AJ, Wang SQ, Zhou SZ 2009 Effect of Al content on

microstructure and mechanical properties of Ti – Al – Si – N nanocomposite coatings Int J Refract Met Hard Mater. 27 718–21. doi:10.1016/j.ijrmhm.2008.12.002.

[22] Varghese V, Ramesh MR, Chakradhar D 2018 Experimental investigation and optimization of machining parameters for sustainable machining. Mater Manuf Process. 33 1782–92. doi:10.1080/10426914.2018.1476760.

[23] She-quan W, Kang-hua C, Li C 2011 Effect of Al and Si additions on microstructure and mechanical properties of TiN coatings J Cent South Univ Technol.18 310–3. doi:10.1007/s11771−011−0696−4.

[24] Barshilia HC, Ghosh M, Shashidhara, Ramakrishna R, Rajam KS 2010. Deposition and characterization of TiAlSiN nanocomposite coatings prepared by reactive pulsed direct current unbalanced magnetron sputtering. Appl Surf Sci. 256 6420–6. doi:10.1016/j.apsusc.2010.04.028.

[25] Chawla V, Jayaganthan R, Chandra R 2010 A study of structural and mechanical properties of sputter deposited nanocomposite Ti–Si–N thin films Vipin. Surf Coat Technol. 204 1582–9.

[26] Ou YX, Chen H, Li ZY, Lin J, Pan W, Lei MK 2018. Microstructure and tribological behavior of TiAlSiN coatings deposited by deep oscillation magnetron sputtering. J Am Ceram Soc. 101 5166–76. doi:10.1111/jace.15769.

[27] Yuan Y, Qin Z, Yu DH, Wang CY, Sui J, Lin H, et al. 2017 Relationship of microstructure, mechanical properties and hardened steel cutting performance of TiSiN-based nanocomposite coated tool. J Manuf Process. 28 399–409. doi:10.1016/j.jmapro.2017.07.007.

[28] Cheng YH, Browne T, Heckerman B, Meletis EI 2010 Mechanical and tribological properties of nanocomposite TiSiN coatings. Surf Coat Technol. 204 2123–9. doi:10.1016/j.surfcoat.2009.11.034.

[29] Wang SQ, Chen L, Yang B, Chang KK, Du Y, Li J, et al. 2010 Effect of Si addition on microstructure and mechanical properties of Ti – Al – N coating RMHM. 28 593–6. doi:10.1016/j.ijrmhm.2010.05.001.

[30] Beake BD, Fox-Rabinovich GS, Veldhuis SC, Goodes SR 2009 Coating optimisation for high speed machining with advanced nanomechanical test methods. Surf Coatings Technol. 203 1919–25. doi:10.1016/j.surfcoat.2009.01.025.

[31] Beake BD, Ning L, Gey C, Veldhuis SC, Komarov A, Weaver A, et al. 2015 Wear performance of different PVD coatings during hard wet end milling of H13 tool steel. Surf Coatings Technol. 279 118–25. doi:10.1016/j.surfcoat.2015.08.038.

[32] N. Fukumoto, H. Ezura TS 2009 Synthesis and oxidation resistance of TiAlSiN and multilayer TiAlSiN/CrAlN coating. Surf Coatings Technol. 204 902–6.

[33] Sivaiah P, Chakradhar D 2017 Comparative evaluations of machining performance during turning of 17-4 PH stainless steel under cryogenic and wet machining conditions. Mach Sci Technol. 22 147–62. doi:10.1080/10910344.2017.1337129.